Nanoscale

MINIREVIEW

Cite this: *Nanoscale*, 2019, **11**, 12449

Ferritin variants: inspirations for rationally designing protein nanocarriers

Yiliang Jin,[a,b] Jiuyang He,[a] Kelong Fan *[a] and Xiyun Yan*[a,b,c]

Received 5th May 2019,
Accepted 7th June 2019

DOI: 10.1039/c9nr03823j

rsc.li/nanoscale

Ferritin, a natural iron storage protein, is endowed with a unique structure, the ability to self-assemble and excellent physicochemical properties. Beyond these, genetic manipulation can easily tune the structure and functions of ferritin nanocages, which further expands the biomedical applications of ferritin. Here, we focus on human H-ferritin, a recently discovered ligand of transferrin receptor 1, to review its derived variants and related structures and properties. We hope this review will provide new insights into how to rationally design versatile protein cage nanocarriers for effective disease treatment.

Introduction

Versatile proteins with distinct structures and functions are produced in the process of natural evolution. Compared with synthesized nanomaterials, natural proteins are endowed with advantages such as low toxicity and high compatibility. Thus, it is becoming more and more popular to utilize naturally occurring proteins in nanomedicine. Among the natural proteins, ferritin, a natural iron storage protein, has been extensively used in the study of diagnosis and therapy of various diseases, including cancer,[1,2] atherosclerosis[3] and rational design of vaccines.[4,5]

Ferritin possesses a unique hollow globular structure. Mammalian ferritin consists of two different subunits, the H-ferritin (HFn) subunit and the L-ferritin (LFn) subunit, with a molecular weight of 21 kDa and 19 kDa, respectively.[6] Interestingly, HFn and LFn can form a 24-mer heteropolymer in any proportion. Moreover, the ratio of H to L subunits varies depending on their original organs and is also affected by pathological conditions.[7]

H and L subunits function distinctively according to their different structures. HFn contains a ferroxidase center and is able to convert free toxic ferrous ions to ferric ions within the protein preventing cells from the damage of the Fenton reaction,[8] while LFn plays an important role in iron nucleation and mineralization. Each ferritin nanocage can accommodate up to 4500 iron atoms,[9] with an iron core formed during the nucleation which is chemically similar to ferrihydrite ($5Fe_2O_3{\cdot}9H_2O$).[10]

[a]*Key Laboratory of Protein and Peptide Pharmaceutical, Institute of Biophysics, Chinese Academy of Sciences, 15 Datun Road, Beijing 100101, China. E-mail: fankelong@ibp.ac.cn; Tel: +86-010-64888256*
[b]*University of Chinese Academy of Sciences, No. 19(A) Yuquan Road, Beijing 100049, China. E-mail: yanxy@ibp.ac.cn; Tel: +86-010-64888583*
[c]*Academy of Medical Sciences, Zhengzhou University, 40 N Daxue Road, Zhengzhou 450052, China*

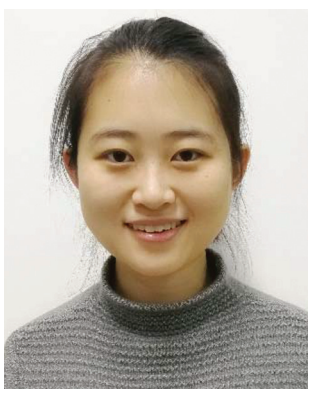

Yiliang Jin

Yiliang Jin obtained her B.S. degree from the College of Pharmacy, Nankai University in 2019. She is currently working on her PhD degree under the supervision of Dr Xiyun Yan at the Institute of Biophysics, Chinese Academy of Sciences. Her research interests focus on ferritin and nanozymes in biomedical applications.

Jiuyang He

Jiuyang He obtained his Bachelor's degree in Biological Science from Jinan University before receiving his Master's degree in Bioengineering in 2015 from Tufts University, where he studied the use of silk protein as a biomaterial for cell culture and RNA stabilization. Currently, he is a doctoral candidate in Prof. Xiyun Yan's group at the University of Chinese Academy of Sciences studying ferritin targeting of diseases.

Ferritin nanocages can be easily modified by genetic or chemical manipulation to introduce additional functionalities. This feature enables ferritin to be a promising platform for biomedical uses. However, a deeper understanding of the structure and properties of HFn is still needed to practically apply HFn to medical applications. In order to investigate the effects of modifications in different regions of HFn, over one hundred HFn variants had been designed in the past few decades. In this review, we summarized the typical recombinant human HFn variants, which we then categorized into three groups – folding and self-assembly, metal transport, ferroxidase activity and iron incorporation according to the properties and biological functions of ferritin. Based on these diverse variants, we further discuss the structure–function relationships of ferritin nanoparticles as well as their potential role as display platforms and attempt at providing a wider perspective on the rational design of ferritin and other protein cage nanocarriers for biomedical uses.

Structure of human HFn

Ferritin, with a hollow spherical structure, has inner and outer diameters of 8 and 12 nm, respectively, consisting of 24 subunits in 4–3–2 symmetry (Fig. 1A). Each monomer of HFn consists of four α-helices (namely A, B, C, and D) and one short helix (namely E) (Fig. 1B).

During self-assembly, four types of interfaces are formed, including the interfaces of six 4-fold axes (C_4 interfaces), eight 3-fold axes (C_3 interfaces), twelve 2-fold axes (C_2 interfaces) and twenty-four C_3–C_4 interfaces (Fig. 1C–F). Each 4-fold channel (hydrophobic) is composed of four short E helices in parallel. And the 3-fold channel (hydrophilic) locates in the joint of C and D helices of three subunits. At the beginning of self-assembly, 24 subunits make up 12 pairs, each subunit of a pair paralleling with the other, head to tail, forming 12 C_2 interfaces. These interfaces are responsible for the nanocage-like structure of HFn formed by 24 subunits *via* self-assembly.[12]

Variants affecting folding and self-assembly

It is crucial to study the folding and self-assembly of a protein so as to understand its biosynthesis, properties and functions. Variants on folding and self-assembly may change the conformation, lattice structure and the oligomerization state of the HFn nanocage (Table 1).

Although amino acid residues at the carboxy terminus (including E-helix) are not essential for the assembly of the 24-mer ferritin nanocage,[13] changes around the 4-fold channel or in the DE loop (GAPESG) can cause conformational changes or aggregation. Cesareni *et al.* have shown that the human HFn nanocage can assemble into two conformation molecules – Flip (the carboxy terminus pointing toward the cavity) and Flop (the carboxy terminus pointing outside) (Fig. 2).[13–15] When Leu169 was substituted by Arg (Variant R2), the hydrophobic nature of the 4-fold channel was altered and resulted in the Flop conformation. Variant F68 (DE loop: ESVWNP) also takes on the Flop conformation. However, none of the six substituted amino acids were identified to be directly responsible for this change. Neither Variant F114 (DE loop: ESVESG) nor F115 (DE loop: GAPWNP) carrying a three-point mutation individually was able to alter the HFn nanocage to assemble in the Flop structure, which means amino acid residues in the DE loop may interact with each other during the folding and self-assembly process.

Variants with positively charged residues at 159, 160, and 161 form an insoluble aggregate.[14] Variant F45 (DE loop: WRKPSL) with positively charged Arg and Lys failed to assem-

Kelong Fan

Dr Kelong Fan received his Ph.D. degree in cell biology from the Institute of Biophysics (IBP), Chinese Academy of Sciences. He is now an associate professor in IBP. His research interests focus on the novel functions and applications of nanozymes and ferritin in biomedicine. He and coworkers discovered for the first time that human H chain ferritin can target and visualize tumor via *binding specifically to a tumor targeting marker transferrin receptor 1. He further employed ferritin as a nanocarrier for antitumor drug delivery. Dr Fan has also made improvements, designs and applications of nanozymes as well.*

Xiyun Yan

Dr Xiyun Yan is a professor at the Institute of Biophysics, a member of the Chinese Academy of Sciences, and the president of the Asian Biophysics Association. Her research interests include studying tumor biology, finding novel targets and developing new methods for tumor theranostics. Dr Yan introduced the concept of "nanozymes" (nanomaterials with enzyme-like characteristics) and used nanoenzymes for tumor diagnosis in combination with ferritin. Her work has been well recognized through honors such as the National Prize for Natural Science and Atlas Award by Elsevier.

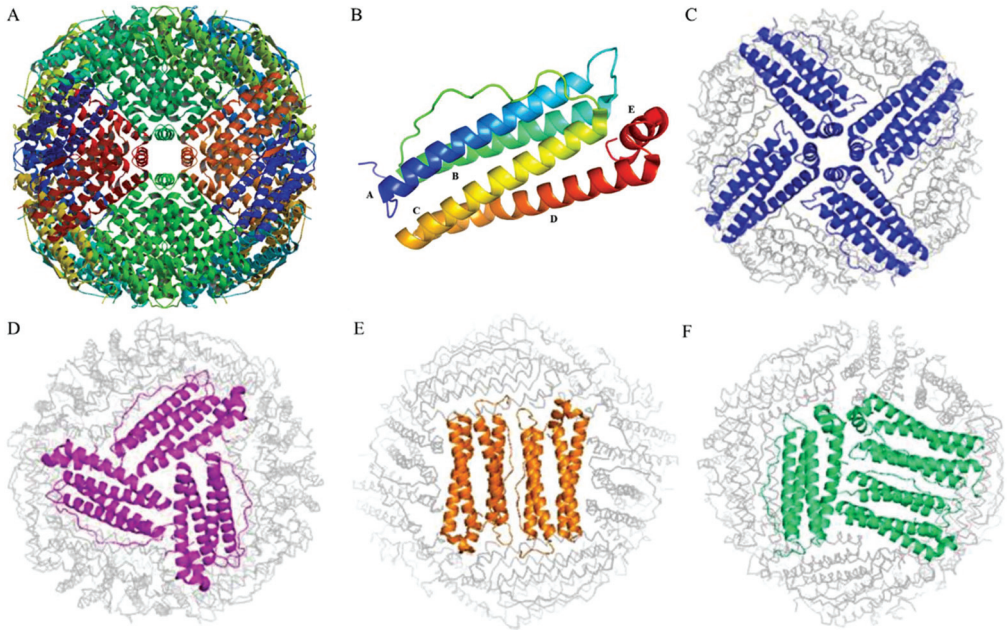

Fig. 1 (A) Structure of wild-type (wt) HFn in 24-mer. (PDB ID: 2FHA) (B) structure of the HFn monomer. The five helixes are labeled accordingly. (C), (D), (E), and (F) Presentation of the four types of interfaces, namely C_4 interfaces, C_3 interfaces, C_2 interfaces and C_3–C_4 interfaces, respectively. They are formed during the self-assembly of ferritin. Adapted from ref. 12. Copyright 2018 American Chemical Society.

Table 1 Human HFn variants involved in folding and self-assembly

Region	Name	Substitutions	Properties	Ref.
C_4 interface	R2 or F29	L169R	Flop conformation	13
DE loop	F68	G159E + A160S + P161V + E162W + S163N + G164P		14 and 15
DE loop	F80	Δ(A160-S163)[a]	Folding and assembling incorrectly	14
	F45	G159W + A160R + P161K + E162P + G164L	Forming an aggregate	14
	F64	G159D + A160N + P161T + E162D + S163L + G164S	Not forming an aggregate	14
	F15	G159R + A160K + P161K + E162A + S163T	Incapable of polymerizing	16
	F16	G159L + A160R + P161K + E162A + S163I + G164T		16
	F38	A160I + P161R + E162A	Precipitation of fully assembled HFn	16
	F62	A160R + P161K + E162P		16
C_3–C_4 interface		Δ(N139-A144)	To form a non-native nanocage in 48-mer or 8-mer	17
		∇(139LNEQVKA)[a]	To form a 16-mer lenticular nanocage	18
		Δ(E134-S182)	To form 8-mer nanorings	12
C_4 interface	F160	Δ(A160-S182)	To widen the 4-fold channel	13, 20 and 21
	S5 or ΔC*	K86Q + C90E + C102A + C130A	Self-assembly in 24-mer	22
C_2 interface	4His-ΔC*	K86Q + C90E + C102A + C130A + L56H + R63H + E67H		22
	MIC1	K86Q + C90E + C102A + C130A + Y39E + N74E + P88A	EDTA: monomer; Cu(II): 24-mer	22
		K86Q + C90E + C102A + C130A + Y39E + N74E + P88A + H173A	EDTA: monomer; Cu(II): 24-mer (only at high protein concentration)	22
		K86Q + C90E + C102A + C130A + Y39E + N74E + P88A + D131A + E134A	EDTA: monomer; Cu(II): 24-mer	22
		K86Q + C90E + C102A + T122H + C130A	To form a bcc lattice	23

[a] Δ for deletion, ∇ for insertion.

ble in a native manner and formed aggregates, while variants with negatively charged amino acid residues such as F64 (DE loop: DNTDLS) do not show the same results. These results indicate that the DE loop is of importance with regard to the assembly of HFn.

DE loop mutations cause the HFn nanocage to form an aggregate by two distinct mechanisms.[16] Some substitutions prevent the polymerization of the monomer. Variant F15 (DE loop: RKKATG) and F16 (DE loop: LRKAIT) cannot fold and assemble in 24-mer while other mutations cause the precipi-

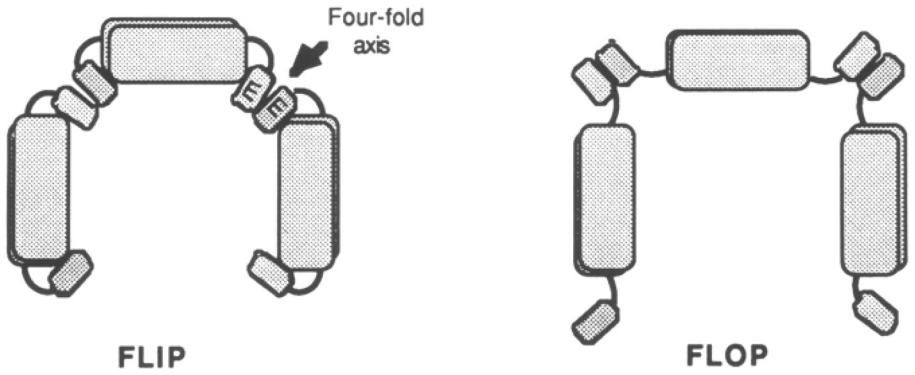

Fig. 2 Schematic representation of the Flip and Flop conformations. Adapted from ref. 13. Copyright 1989 John Wiley and Sons.

tation of fully assembled HFn such as Variant F38 (DE loop: GIRASG) and F62 (DE loop: GRKPSG).

Inter-subunit interfaces are responsible for the self-assembly of ferritin. The structure and oligomerization state of HFn can be altered by selectively eliminating or introducing amino acid residues on different kinds of interfaces. Notably, modifications on the C_3–C_4 interfaces and C_2 interfaces have a direct impact on the self-assembly of HFn. Zhang *et al.* have introduced a novel strategy on engineering protein interfaces termed key subunit interface redesign (KSIR).[17] This new method includes deletion of a certain number of "silent" amino acid residues on the interfaces, which are not involved in the interfacial interactions as well as the process of self-assembly. By eliminating six amino acid residues (sequence: 139NEQVKA) on the C_3–C_4 interface, two subunits are produced named H_α and H_β, respectively, both of which are obtained from one polypeptide. In essence, the newly formed sequence folds into two distinct conformations – H_α does not contain the E-helix structure while H_β lacks the CD turn. This novel non-native protein cage of 17 nm in the crystal is a heteropolymer of 48 subunits consisting of H_α and H_β at a ratio of 1 : 1 (Fig. 3A). Interestingly, the oligomerization state varies under different experimental conditions as the 48-mer HFn nanocage converts into its 8-mer analogue in solution (50 mM Tris-HCl, pH 8.0). In another case, seven extra "silent" amino acid residues (sequence: 139LNEQVKA) were introduced on the C_3–C_4 interface, resulting in a lenticular 10 nm × 8 nm ferritin nanocage composed of two new types of subunits in different conformations termed H'_α and H'_β, respectively.[18] One end of the D-helix near the C-terminus moves to the C-terminus resulting in the H'_α subunit, and the other end of the D-helix close to the N-terminus moves to the N-terminus producing H'_β. This non-native protein cage is composed of 16 subunits of H'_α and H'_β at a ratio of 1 : 1 (Fig. 3B). The 16-mer nanocage shows ferroxidase activity parallel to that of wild-type HFn. The wild-type ferritin nanocage remains stable under strongly acidic conditions (pH 3.4) and disassembles into subunits at pH 2.0.[19] However, this HFn nanocage variant is pH-responsive as it disassembles at pH 3.0 and reassembles at pH 7.5, capable of encapsulating curcumin in its cavity,

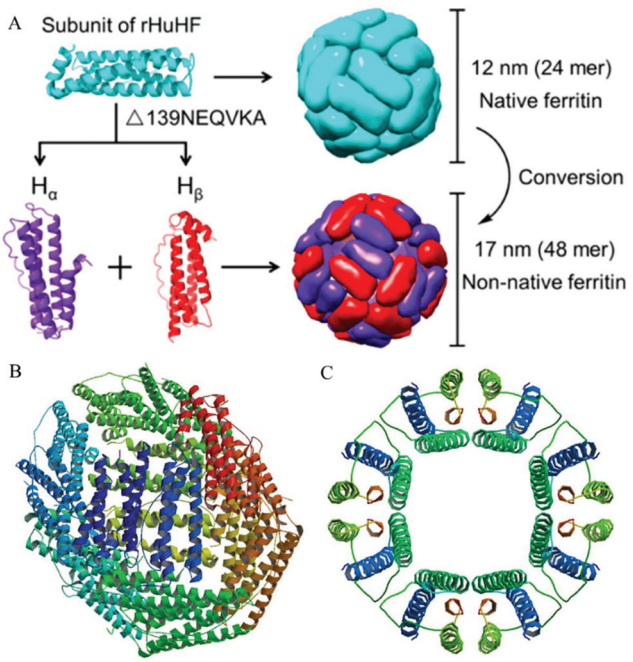

Fig. 3 (A) Presentation of the conversion of native HFn into its 48-mer analogue in the crystal. Adapted from ref. 17. Copyright 2016 American Chemical Society. (B) Illustration of the lenticular structure of 16-mer HFn. (PDB ID: 5GOU). (C) Illustration of the 8-mer nanoring. (PDB ID: 5ZND).

suggesting that this variant may function as a promising nanocarrier for acid-sensitive drugs.

To investigate the strategy for developing novel patterns of assemblies, Wang *et al.* have designed a new variant with 49 residues at the carboxy terminus eliminated (C_3–C_4 interface) which resulted in the formation of 8-mer nanorings instead of a 24-mer nanocage (Fig. 3C).[12] This newly formed HFn nanoring variant exhibits a cylindrical structure with a height of 5.1 nm as well as inner and outer diameters of 3.2 and 7.0 nm, respectively. These successful designs suggest that the folding and self-assembly of HFn may become controllable by engin-

eering the key interfaces and they may provide a novel approach for engineering different types of assemblies.

Luzzago *et al.* have verified that Variant F160 (deletion of amino acid residues from position 160 to 182) does not affect the formation of the nanocage,[13] whereas the 4-fold channel is widened by eliminating the last 23 amino acid residues including the E-helix and DE turn. Moreover, Chen *et al.* have found that this variant disassembles at pH 4.0 and reassembles at pH 7.5.[20] The disassembly pH value of Variant F160 is higher than that of wild-type HFn, suggesting that small molecule drugs sensitive to pH are more suitable to be encapsulated within the nanocage of the HFn complex.[20] Each engineered HFn nanocage variant is capable of encapsulating 14 molecules of curcumin within its cavity during the process of disassembly and reassembly of the protein cage, suggesting that Variant F160 may function as a promising nanocarrier in the future.

Ahn *et al.* have designed 4-fold channel-nicked human HFn nanocages as novel nanocarriers.[21] Nicked HFn nanocages consist of wild-type HFn and F160 at mixing ratios of 1 : 1–2 : 1 (wt : F160). They also developed a new method of drug uptake and release based on ferritin by making use of the natural characteristic of ferritin to combine metal ions and to disassemble/assemble according to pH. The nicked HFn nanocages were engineered *via* a pH-responsive disassembly/assembly approach first, and then Fe(II)-conjugated drugs were utilized so that they can be easily encapsulated by simple incubation. As a result, one nicked HFn nanocage is capable of accommodating about 121 molecules of doxorubicin (Dox) *via* Fe(II)-mediated loading, which can be released within 5 hours at pH 4 in a tumor acidic microenvironment (the new HFn complexes disassemble at pH 4–5) and the encapsulated drug molecules are as effective as free Dox molecules at a cellular level. This novel design of HFn variants may become an alternative strategy for effective drug loading.

To control the assembly process of HFn, Huard *et al.* have introduced a new method, reverse metal-templated interface redesign (rMeTIR) (Fig. 4).[22] Variant ΔC* (K86Q + C90E + C102A + C130A) lacks all cysteine residues yet is still capable of self-assembling into 24-mer and was used as a control. Variant 4His-ΔC* (K86Q + C90E + C102A + C130A + L56H + R63H + E67H) can also form 24-mer like the native HFn nanocage, despite substituting out three of the residues which play an important role in hydrogen-bonding interactions and are located at the C_2 interface of the HFn nanocage. Further substitutions that are involved at the C_2 interface have been made to interfere with the normal assembly process. Variant MIC1 (K86Q + C90E + C102A + C130A + Y39E + N74E + P88A) remains in a monomer state with EDTA, but forms 24-mer in the presence of Cu(II). Polymerization of ferritin may become controllable with this copper-mediated approach.

Aside from the conformation and oligomerization state, the lattice structure of ferritin can also be altered *via* genetic modification. K86Q is commonly designed to enable crystallization of ferritin in a face-centered cubic (fcc) lattice.[11] However, when T122H is introduced in Variant CdM (K86Q) as well as C90E, C102A, C130A, ferritin nanocages can self-assemble in a body-centered cubic (bcc) lattice (Fig. 5).[23] The construction of this variant is accomplished through a metal–organic linker-directed strategy. Zn^{2+} ions are bound to the sites exposed on the exterior surface of the engineered ferritin, meanwhile benzohydroxamic acids are employed as organic linkers to help form the expected 3D lattice structure.

Variants affecting metal transport

Magneto-ferritin (M-HFn) has been demonstrated to be a powerful tool in the studies of various disease diagnosis, including atherosclerosis,[3,24] tumor imaging[25,26] and detection.[27,28] Biomimetic synthesis of M-HFn relies on the iron metal entry channels on the ferritin nanocage. In fact, various metal ions such as Cu^{2+}, Mn^{2+}, and Co^{2+} have been successfully encapsulated into ferritins *via* simple diffusion[29] which provides novel approaches for effective accommodation of organic complexes. As mentioned before, Dox molecules can be encapsulated into the 4-fold channel-nicked human HFn variant *via* the Fe(II)-mediated strategy.[21] Aside from that, Dox can also be loaded onto a Cys-Asp-Cys-Arg-Gly-Asp-Cys-Phe-Cys (RGD4C)-modified ferritin variant *via* a Cu(II)-assisted approach.[30] In this case, Dox molecules were precomplexed with Cu(II) which can be encapsulated into RGD4C-ferritin variant nanocages presumably on the metal binding sites of the 3-fold channel. However, it is still controversial whether Dox molecules (>500 Da) can traverse such narrow pathways, hence further research is needed.

HFn plays an important role in iron metabolism, thus the metal transport of HFn should be considered in the rational design of ferritin nanocarriers. In order to identify the pathway of iron and other metal incorporation, several mutations designed on the 3-fold channel were reported (Table 2).

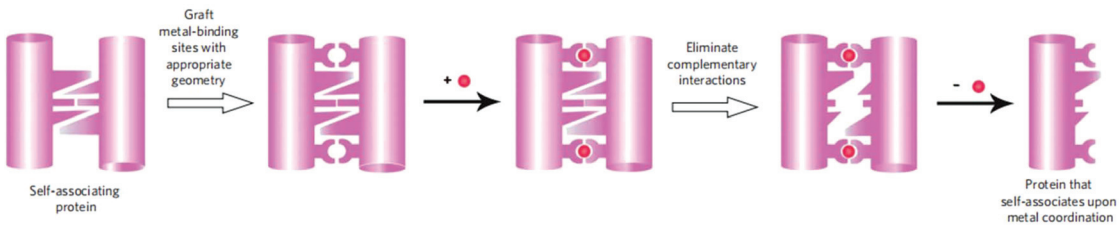

Fig. 4 Scheme of rMeTIR. Adapted from ref. 22. Copyright 2013 Springer Nature.

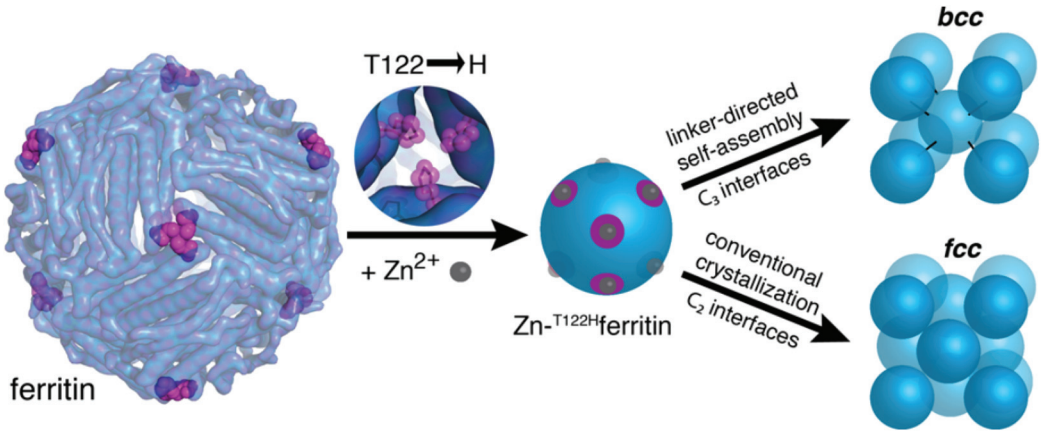

Fig. 5 Scheme of the linker-directed self-assembly of human HFn into a bcc lattice. Adapted from ref. 23. Copyright 2015 American Chemical Society.

Table 2 Human HFn variants involved in the metal transport

Region	Name	Substitutions	Properties	Ref.
3-Fold channel	174	K86Q + D131H	Inhibiting the entry of Fe(II)	41 and 42
	175	K86Q + D131H + E134H	Alteration of the channel	42
	204	K86Q + E134A	Inhibiting the entry of Fe(II)	41 and 42
	206	K86Q + D131A + E134A		31 and 42
	S14	D131I + E134F	Lower speed of Fe(II) uptake	32
		E140A	Delay in the oxidation and nucleation	43
		E140Q	rate	43
	H8	H13D + E64C + C90R + C102A + H105Q + E140C + K143C + E147C	To form stable noble metal nanoparticles within the cavity	40

Asp131 and Glu134 are located at the 3-fold channel of ferritin, where the metal is predicted to be transported in and out of ferritin. When hydrophilic Asp and Glu are substituted by hydrophobic Ala (Variant 206), ferrous ions are inhibited from binding the 3-fold channel.[31] In the same manner, Variant S14 (D131I + E134F) reduces the transport rate of Fe(II) into the cavity by virtue of the introduction of hydrophobic Ile and Phe, which also narrows the channel.[32] These results suggest that the hydrophilicity of the 3-fold channel is a requisite for metal transit.

Masuda *et al.* have prepared Variants E140A and E140Q to evaluate the significance of the conserved transit sites of human HFn.[33] Both variants were obtained by crystallization similar to wild-type HFn without the introduction of K86Q. They exhibit delay in the oxidation and nucleation, and the reaction rate of E140Q is slower than that of E140A.

It is well accepted that Fe(II) reaches the ferroxidase site through the 3-fold channel of vertebrate ferritin.[34,35] Additionally, Theil *et al.* have identified the importance of Glu57 and Glu136 for Fe(II) transit in frog ferritin.[36] These conserved carboxylate residues between the channels and ferroxidase sites guide the Fe^{2+} ions to the catalytic centers of ferritin.

In recent years, by means of nuclear magnetic resonance (NMR) approaches, high resolution X-ray absorption spectroscopic analysis *etc.*, the iron pathway and transfer process of ferritin of various species have been studied and more details have been revealed.[37–39] To sum up, the iron pathway of human HFn is presumedly as follows. Ferrous ions are captured by Glu134 first and then guided to Asp131, after which they are transported to Thr135 and His136, and then to the conserved site Glu140 in succession. Fe(II) ions are guided to Glu61 and Gln58 by the side chain of Glu140 before ultimately reaching the ferroxidase center.[33]

Butts *et al.* have designed a novel HFn variant for directing noble metal ions into the cavity of the HFn protein shell.[40] Cysteines have been found to be critical ligands for noble metal ions such as Hg^{2+} and Au^{3+}. In variant H8 (H13D + E64C + C90R + C102A + H105Q + E140C + K143C + E147C), a total of 96 cysteines and histidines are removed from the outer space of the HFn nanocage and 96 non-native cysteines are introduced into the inner cavity. This newly engineered variant displays similar stability to that of wild-type ferritin but is more likely to form noble metal nanoparticles in its cavity.

Variants affecting the ferroxidase activity and iron incorporation

In the last century, scientists focused more on the functional properties of ferritins and managed to identify the critical amino acids of HFn which had a direct influence on the ferrox-

Table 3 Human HFn variants which are related to the ferroxidase ability and iron incorporation of HFn

Region	Name	Substitutions	Properties	Ref.
Ferroxidase center	222	K86Q + E62K + H65G	Loss of ferroxidase activity	58
		K86Q + E27A	Exhibiting little ferroxidase activity	45 and 46
		K86Q + E107A		45
		K86Q + E27D	Ferroxidase activity is slightly improved	44
		K86Q + E107D	Loss of ferroxidase activity	44
		K86Q + E27D + 107D		44
		K86Q + Y34F	Weaker binding and oxidation of Fe(II)	45 and 46
3-Fold channel	204	K86Q + E134A	Less iron incorporation	32 and 45
	175	K86Q + D131H + E134H	Oxidation rates decrease greatly	45
	206	K86Q + D131A + E134A	Oxidation rates decrease greatly & iron incorporation decreases	32 and 45
	F100	E62K + H65G + D131A + E134A	Greatly decreased	32
	S15	E62H + D131I + E134F	Loss of ferroxidase activity & less iron incorporation	32
	S14	D131I + E134F	Weaker ferroxidase activity & a decrease of iron incorporation	32
Around the 3-fold channel	S5	K86Q + C90E + C102A + C130A	Less efficient in iron incorporation	32
	S9	K86Q + H118A		32
	S10	K86Q + H128A	More efficient in iron incorporation	32
Cavity	A2	E61A + E64A + E67A	Decrease of iron incorporation	31 and 49
	A1	E64A + E67A	Similar to wild-type HFn	49
	S8	K86Q + H57E + H60E	No obvious effect or a slight increase in mineralization efficiency	32 and 50
		K86Q + E61A	Preventing iron binding	52
		L138P	The rate of iron release increases	51
Ferroxidase center & cavity	A222	K86Q + E62K + H65G + E61A + E64A + E67A	Loss of ferroxidase activity & iron incorporation greatly decreases	41
	S1	K86Q + E62K + H65G + E61A + E64A + E67A + D42A	Loss of ferroxidase activity & loss of iron incorporation	52
		C90R C102A C130A C90R + C102A C90R + C102A + C130A	C90R and C102A substitutions decrease the amount of aggregates formed during the iron loading process.	53

idase ability and iron incorporation. Some of them are shown in Table 3.

Glu62 and Glu65 are essential to the Fe(II) oxidation reaction. When they are substituted in Variant 222 (K86Q + E62K + H65G), ferroxidase ability disappears completely. Toussaint *et al.*[44] found that when Glu27 is substituted by Asp (E27D), the variant exhibits comparable ferroxidase activity to wild-type ferritin mainly because it binds to two metal ions in the ferroxidase center. However, variants carrying E107D or both E27D and E107D do not show ferroxidase activity at all due to their failure to complex two atoms correctly. Variants carrying substitution of E27A or E107A show little ferroxidase activity while the activity of Variant (K86Q + E27D) is slightly improved.[44,45] Treffry *et al.*[46] have found that the binding and oxidation of Fe(II) could be affected when Tyr34 (located near the site B) is substituted by Phe (Y34F). In fact, it was well accepted that there are two iron ion binding sites in the ferroxidase center of human HFn, termed Fe1 and Fe2, respectively. Fe1 is coordinated by Glu27, His65 and Glu62 while Glu62 and Glu107 contribute to Fe2 (Fig. 6).[33,44,47] Pozzi and co-workers identified additional two binding sites (Fe3 and Fe4) in the ferroxidase center where Gln58, Glu61 and His57 are involved in the coordination of iron ions.[48]

Mutations on the 3-fold channel or around it may have an impact on the ferroxidase activity. As the narrowest part of the 3-fold channel, Asp131 and Glu134 are of great importance in the process of iron uptake. Variant 204 (K86Q + E134A) has little effect on the oxidation rates compared with Variant CdM

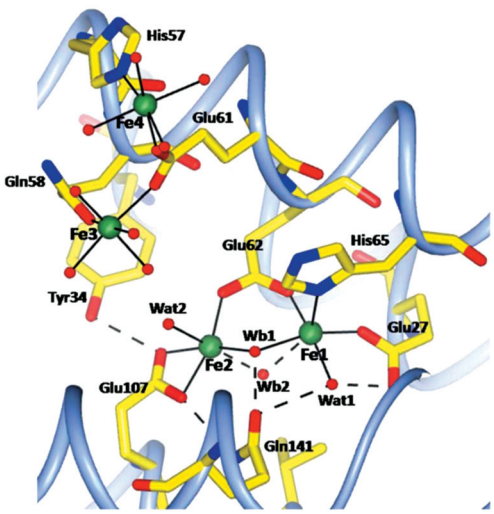

Fig. 6 Schematic representation of the ferroxidase sites of human HFn. Wat, water molecules; Wb, water/hydroxide molecules. Adapted from ref. 48. Copyright 2015 WILEY-BLACKWELL.

(K86Q), but the Fe(II) oxidation rates decrease obviously when it comes to variants bearing two changes in the narrowest part of the 3-fold channel.[45] The oxidation rate of Variant 175 (K86Q + D131H + E134H) is a bit greater than Variant 206 (K86Q + D131A + E134A) possibly because the hydrophilic nature of the 3-fold channel is not altered. Variants carrying

two substitutions on the 3-fold channel exhibit weaker ferroxidase activity due to the low speed of the transport of Fe(II) into the cavity. These variants do not prevent iron from entering the cavity, but the amount of iron incorporated is much greater in wild-type HFn.

Mutations around the 3-fold channel can also have an impact on the iron incorporation. Variant S10 (K86Q + H128A) can facilitate the process of iron binding while Variant S9 (K86Q + H118A) suppresses it.[32]

Glu61, Glu64 and Glu67 of HFn are considered as the nucleation centers of ferrihydrite. In Variant A2 (E61A + E64A + E67A), all of them are replaced by alanine, therefore iron binding is inhibited.[31] These substitutions of E61A, E64A and E67A also decrease the oxidation rate greatly at the same time.[32] Bou-Abdallah *et al.* reported that the impaired iron oxidation and mineralization contribute to the disruption of Glu61 which functions as a ferroxidase site in human HFn.[49] This conclusion was based on the fact that Variant A1 (E64A + E67A) shows ferroxidase activity and iron incorporation close to that of wild-type human HFn. In addition, Variant S8 (K86Q + H57E + H60E) may be a little more efficient during the process of iron mineralization.[50] Pore mutation L138P increases the rate of iron release greatly compared with wild-type HFn.[51]

With both ferroxidase and nucleation center altered, Variant A222 (K86Q + E62K + H65G + E61A + E64A + E67A) exhibits no ferroxidase activity and the capacity of iron incorporation decreases greatly.[41] When an additional change of D42A is introduced, Variant S1 (K86Q + E62K + H65G + E61A + E64A + E67A + D42A) completely loses the ability of iron binding.[52]

Cysteine residues in HFn sequences (located at positions 90, 102 and 130) also play an important role in the process of iron nucleation. Cys90, in the end of the BC loop, is critical for the formation of an HFn aggregate during iron loading *via* its ferroxidase activity because it is oxidized in the process.[53] HFn with C90R substitution is less likely to form an aggregate, and so is HFn with C102A substitution. Variants with both C90R and C102A changes cause the least aggregation. However, it is surprisingly noted that the ferroxidase activity of these variants is the same.

At low iron levels, ferrous ions react with oxygen first at a ratio of 2 : 1 at ferroxidase sites generating hydrogen peroxide.[54] The reaction results in an intermediate blue product diferric peroxo (DFP) which finally decays to μ-1,2-oxodiferric species.[55] The diferric products migrate through the nucleation pathways, the exits of which are clustered around the 4-fold channels.[56] Consequently, they enter the internal cavity and form an iron core accomplishing the mineralization process. At higher iron levels, Fe(II) ions can be directly oxidized on the emerging iron core and the ratio of iron to oxygen is 4 : 1 in the overall reaction.[29] In the presence of excess O_2, the observed iron oxidation reactions did not obey Michaelis–Menten kinetics whereas at low O_2 concentration similar to the physiological conditions, iron uptake kinetics exhibited Michaelis–Menten behavior.[57]

Potential role of Ferritin as nanocarriers

HFn nanocages possess the following special features: (1) it can disassemble at pH 2.0 or 8 M urea and resemble in a neutral environment;[19,59] (2) it can remain stable at high temperatures (80 °C); (3) moreover, HFn is found to bind specifically to human transferrin receptor-1 (TfR1),[60] and the latter is overexpressed in tumor cells,[61] which means HFn may become useful in targeted drug delivery in the treatment of tumor. Simply put, the reversible disassembly/assembly, thermostability and intrinsic targeting make HFn a suitable nanocage for drug delivery and other biomedical applications. Moreover, a HFn nanocage is a promising chamber for small molecule drugs such as doxorubicin,[62] curcumin,[63] cisplatin[64] *etc*. It encapsulates drugs primarily by means of pH-dependent or urea dependent disassembly/reassembly of the HFn nanocage. These engineered nanocarriers may be further applied in cancer theranostics from bench to bedside. Some reviews have summarized the potential of HFn as a biological platform,[29,65–67] however, there is a limitation that some drugs are unstable under strongly acidic conditions or high concentrations of urea, so a new strategy for utilizing HFn as nanocarriers needs to be further considered.

The ferritin nanocages can be easily engineered *via* genetic manipulation or chemical modification. So far, four primary schemes for display on ferritin (including but not limited to human HFn) have been employed: display on the N-terminal, DE loop, and the 3-fold channel, deletion of the E helix and then display on the C-terminal. Particularly, these strategies can also be used in combination. Recently, our group displayed a SP94 peptide on the N-terminal of *Pyrococcus furiosus* ferritin targeting hepatocellular carcinoma cells.[68,69] Besides, the interleukin-4 receptor (IL-4R)-targeting peptide, AP-1, was genetically introduced into the DE loop of human LFn by the Kim group to enhance the affinity of peptide ligands for the treatment of asthma.[70] Furthermore, they also devised peptides displayed on the human LFn nanocage of bi-specificity or superaffinity *via* two-site (N-terminal and the DE loop) display.[71] Kim *et al.* had designed a double-chambered human HFn platform based on the E helix-deficient ferritin (short ferritin), of which both the N- and C-terminal sites functioned as display platforms.[72] A pro-apoptotic peptide $CGKRK(KLAKLAK)_2$ targeting tumor was introduced on the N-terminal while green fluorescent protein (GFP) was displayed on the C-terminal of human HFn. Moreover, our group developed a fenobody platform where nanobodies can be displayed on the C-terminal of E helix-deficient *Pyrococcus furiosus* ferritin.[73] With the rapid development of new vaccines, numerous nanoparticle-based vaccines have been designed. Due to its unique structure of the 3-fold channel, ferritin may be applied in displaying viral antigens. Kanekiyo and coworkers found that influenza virus haemagglutinin could be inserted into the 3-fold axis of *Helicobacter pylori* ferritin and trigger broader immune responses.[74] These novel ferritin variants with additional targets and high avidity may play an important role in future

biomedical applications and further explorations need to be done.

Interestingly, human ferritin protein amyloid fibrils possess a double stranded twisted ribbon structure and display chirality.[75] HFn shows mainly left-handed chirality whereas LFn usually shows right-handed chirality. It is possible that chiral molecules can be designed by re-engineering the primary structure of ferritin.

As is described before, HFn nanocage variants can be engineered *via* a new strategy based on inter-subunit redesigns.[18] In turn, other structurally similar protein nanocages could be converted into HFn analogues under certain conditions. In a recent study, an 8-mer protein architecture (namely NF-8) was used as a template to produce three distinct nanocages with different geometries mediated by intra- or inter-subunit disulfide bonds.[76] Ferritin-like nanocages were generated from the bowl-like NF-8 by deleting an intra-subunit S–S while selectively inserting an inter-subunit S–S of NF-8 results in a 16-mer lenticular nanocage. Besides, combined with these two procedures, a 48-mer nanocage could form in solution. Accordingly, rational designs of ferritin and its variants may become achievable in the near future by engineering the interfaces of ferritin.

Perspectives

HFn is capable of self-assembling into a spherical structure. A number of variants have been engineered to investigate the structure and properties of human HFn. The structure determines the function, which is, the amino acid sequence and the tertiary structure of HFn can affect its self-assembly, ferroxidase activity, metal accommodation and storage capacity, which may provide new insights into the rational design of protein cage nanocarriers. As a prototypical protein cage nanoparticle, ferritin potentially serves as display and delivery platforms. With peptides or small molecules (drugs, contrast agents, *etc*.) introduced, engineered ferritin complexes can be favored with various functionalities such as targeting and high affinity, which makes them ideal nanocarriers in targeted drug delivery, diagnosis and therapy.

In recent years, protein-based nanoparticles in biomedical applications have aroused much interest. Among them, rational designs of protein nanocarriers are of great importance. As future perspectives, we will also present some ideas for inspiration in designing ferritin-based or other protein nano-formulations.

First of all, noting the special features of ferritin and its derived variants, ferritin nanocarriers can be designed on the basis of the spatial structure or conformation and biological activity *via* genetic engineering. For example, based on the Flop conformation of HFn, targeting moieties can be displayed on the 4-fold axis and the 4-bundles of ligands can mimic some natural structures or enhance the avidity of ligands in biomedical uses. Besides, ferritin nanocages without the capability of accommodating iron may function as a better nanocarrier. These variants will not affect the iron homeostasis after entering human organism, avoiding the potential adverse effects on the human body. Therefore, iron incorporation deficient ferritin platforms are most likely to fulfill the requirement of nanocarriers. Moreover, the size and geometries of ferritin may be controlled by modifying certain types of interfaces since non-native ferritin nanocages with different states of oligomerization have emerged. These newly formed variants may possess larger cavity and are accessible to accommodate more molecules, which may provide new ideas for designing nanocarriers.

Secondly, additional functionalities can be introduced on ferritin by genetic or chemical approaches. Targeting peptides, fluorescent proteins, viral antigens and other ingredients can be displayed on ferritin platforms. As an endogenous protein, biocompatible ferritin platforms may function as drug carriers or vaccine vectors in disease theranostics. As we introduced before, tumor-targeting moieties can be displayed on ferritin cages and small molecule drugs are capable of being encapsulated in the cavity of ferritin *via* disassembly/assembly or simple incubation. Peptide bunches can be designed and oblige ferritin platforms with high avidity and targeting activity. Moreover, it is intriguing that some viral antigens were reported to be displayed in the 3-fold channel of ferritin.[4,74,77–79] In the near future, self-assembling protein cages may play an important role in structure-based vaccine design.

Finally, designs of other protein-based nanocarriers may be inspired by ferritin nanocage platforms. Protein cages such as heat-shock proteins,[80] E2 protein,[81] bacteriophage Qβ[82] *etc*. are also promising nanocarriers, some of which are capable of self-assembling as well. By thoroughly investigating the structure–function relationship of these protein nanoparticles (*e.g.* by engineering variants and finding out the critical amino acids and interfaces), we may have a better understanding and hence devise rational nanocarriers for biomedical applications.

Therefore, it is essential to explore how to design ferritin-based nanocarriers and apply them in biomedicine. We expect that ferritin and other protein cages may be employed from bench to bedside in the near future.

Conflicts of interest

There are no conflicts to declare.

Acknowledgements

This work was financially supported by the National Natural Science Foundation of China (No. 31871005, 31530026), the Chinese Academy of Sciences under Grant No. YJKYYQ20180048, the Strategic Priority Research Program of the Chinese Academy of Sciences (XDPB29040101), the National Key Research and Development Program of China

(No. 2017YFA0205200) and the Youth Innovation Promotion Association CAS (2019093).

References

1 M. Truffi, L. Fiandra, L. Sorrentino, M. Monieri, F. Corsi and S. Mazzucchelli, *Pharmacol. Res.*, 2016, **107**, 57–65.

2 K. Fan and X. Yan, in *Handbook of Nanomaterials for Cancer Theranostics*, ed. J. Conde, Elsevier, 2018, pp. 143–175, DOI: 10.1016/B978-0-12-813339-2.00006-2.

3 M. Liang, H. Tan, J. Zhou, T. Wang, D. Duan, K. Fan, J. He, D. Cheng, H. Shi, H. S. Choi and X. Yan, *ACS Nano*, 2018, **12**, 9300–9308.

4 H. M. Yassine, J. C. Boyington, P. M. McTamney, C. J. Wei, M. Kanekiyo, W. P. Kong, J. R. Gallagher, L. Wang, Y. Zhang, M. G. Joyce, D. Lingwood, S. M. Moin, H. Andersen, Y. Okuno, S. S. Rao, A. K. Harris, P. D. Kwong, J. R. Mascola, G. J. Nabel and B. S. Graham, *Nat. Med.*, 2015, **21**, 1065–1070.

5 Z. Wang, L. Xu, H. Yu, P. Lv, Z. Lei, Y. Zeng, G. Liu and T. Cheng, *Biomater. Sci.*, 2019, **7**, 1794–1800.

6 P. Arosio, T. G. Adelman and J. W. Drysdale, *J. Biol. Chem.*, 1978, **253**, 4451–4458.

7 F. M. Torti and S. V. Torti, *Blood*, 2002, **99**, 3505–3516.

8 P. Arosio, R. Ingrassia and P. Cavadini, *Biochim. Biophys. Acta*, 2009, **1790**, 589–599.

9 S. C. Andrews, P. Arosio, W. Bottke, J. F. Briat, M. von Darl, P. M. Harrison, J. P. Laulhere, S. Levi, S. Lobreaux and S. J. Yewdall, *J. Inorg. Biochem.*, 1992, **47**, 161–174.

10 S. Mann, J. V. Bannister and R. J. Williams, *J. Mol. Biol.*, 1986, **188**, 225–232.

11 D. M. Lawson, P. J. Artymiuk, S. J. Yewdall, J. M. Smith, J. C. Livingstone, A. Treffry, A. Luzzago, S. Levi, P. Arosio, G. Cesareni, *et al.*, *Nature*, 1991, **349**, 541–544.

12 W. Wang, L. Wang, H. Chen, J. Zang, X. Zhao, G. Zhao and H. Wang, *J. Am. Chem. Soc.*, 2018, **140**, 14078–14081.

13 A. Luzzago and G. Cesareni, *EMBO J.*, 1989, **8**, 569–576.

14 R. Jappelli, A. Luzzago, P. Tataseo, I. Pernice and G. Cesareni, *J. Mol. Biol.*, 1992, **227**, 532–543.

15 R. Jappelli and G. Cesareni, *Biochem. Biophys. Res. Commun.*, 1998, **250**, 342–346.

16 R. Jappelli and G. Cesareni, *FEBS Lett.*, 1996, **394**, 311–315.

17 S. Zhang, J. Zang, X. Zhang, H. Chen, B. Mikami and G. Zhao, *ACS Nano*, 2016, **10**, 10382–10388.

18 S. Zhang, J. Zang, W. Wang, H. Chen, X. Zhang, F. Wang, H. Wang and G. Zhao, *Angew. Chem., Int. Ed.*, 2016, **55**, 16064–16070.

19 M. Kim, Y. Rho, K. S. Jin, B. Ahn, S. Jung, H. Kim and M. Ree, *Biomacromolecules*, 2011, **12**, 1629–1640.

20 H. Chen, S. Zhang, C. Xu and G. Zhao, *Chem. Commun.*, 2016, **52**, 7402–7405.

21 B. Ahn, S. G. Lee, H. R. Yoon, J. M. Lee, H. J. Oh, H. M. Kim and Y. Jung, *Angew. Chem., Int. Ed.*, 2018, **57**, 2909–2913.

22 D. J. Huard, K. M. Kane and F. A. Tezcan, *Nat. Chem. Biol.*, 2013, **9**, 169–176.

23 P. A. Sontz, J. B. Bailey, S. Ahn and F. A. Tezcan, *J. Am. Chem. Soc.*, 2015, **137**, 11598–11601.

24 T. Wang, J. He, D. Duan, B. Jiang, P. Wang, K. Fan, M. Liang and X. Yan, *Nano Res.*, 2019, **12**, 863–868.

25 Y. Zhao, M. Liang, X. Li, K. Fan, J. Xiao, Y. Li, H. Shi, F. Wang, H. S. Choi, D. Cheng and X. Yan, *ACS Nano*, 2016, **10**, 4184–4191.

26 C. Cao, X. Wang, Y. Cai, L. Sun, L. Tian, H. Wu, X. He, H. Lei, W. Liu, G. Chen, R. Zhu and Y. Pan, *Adv. Mater.*, 2014, **26**, 2566–2571.

27 K. Fan, C. Cao, Y. Pan, D. Lu, D. Yang, J. Feng, L. Song, M. Liang and X. Yan, *Nat. Nanotechnol.*, 2012, **7**, 459–464.

28 Y. Du, K. Fan, H. Zhang, L. Li, P. Wang, J. He, S. Ding, X. Yan and J. Tian, *Nanomedicine*, 2018, **14**, 2259–2270.

29 G. Jutz, P. van Rijn, B. Santos Miranda and A. Boker, *Chem. Rev.*, 2015, **115**, 1653–1701.

30 Z. Zhen, W. Tang, H. Chen, X. Lin, T. Todd, G. Wang, T. Cowger, X. Chen and J. Xie, *ACS Nano*, 2013, **7**, 4830–4837.

31 E. R. Bauminger, P. M. Harrison, D. Hechel, I. Nowik and A. Treffry, *Biochim. Biophys. Acta*, 1991, **1118**, 48–58.

32 S. Levi, P. Santambrogio, B. Corsi, A. Cozzi and P. Arosio, *Biochem. J.*, 1996, **317**, 467–473.

33 T. Masuda, F. Goto, T. Yoshihara and B. Mikami, *Biochem. Biophys. Res. Commun.*, 2010, **400**, 94–99.

34 E. C. Theil, R. K. Behera and T. Tosha, *Coord. Chem. Rev.*, 2013, **257**, 579–586.

35 J. M. Bradley, G. R. Moore and N. E. Le Brun, *Curr. Opin. Chem. Biol.*, 2017, **37**, 122–128.

36 R. K. Behera and E. C. Theil, *Proc. Natl. Acad. Sci. U. S. A.*, 2014, **111**, 7925–7930.

37 P. Turano, D. Lalli, I. C. Felli, E. C. Theil and I. Bertini, *Proc. Natl. Acad. Sci. U. S. A.*, 2010, **107**, 545–550.

38 D. Lalli and P. Turano, *Acc. Chem. Res.*, 2013, **46**, 2676–2685.

39 C. Pozzi, F. Di Pisa, D. Lalli, C. Rosa, E. Theil, P. Turano and S. Mangani, *Acta Crystallogr., Sect. D: Biol. Crystallogr.*, 2015, **71**, 941–953.

40 C. A. Butts, J. Swift, S.-G. Kang, L. Di Costanzo, D. W. Christianson, J. G. Saven and I. J. Dmochowski, *Biochemistry*, 2008, **47**, 12729–12739.

41 V. J. Wade, S. Levi, P. Arosio, A. Treffry, P. M. Harrison and S. Mann, *J. Mol. Biol.*, 1991, **221**, 1443–1452.

42 A. Treffry, P. M. Harrison, A. Luzzago and G. Cesareni, *FEBS Lett.*, 1989, **247**, 268–272.

43 T. Masuda, F. Goto, T. Yoshihara and B. Mikami, *Biochem. Biophys. Res. Commun.*, 2010, **400**, 94–99.

44 L. Toussaint, L. Bertrand, L. Hue, R. R. Crichton and J.-P. Declercq, *J. Mol. Biol.*, 2006, **365**, 440–452.

45 A. Treffry, E. R. Bauminger, D. Hechel, N. W. Hodson, I. Nowik, S. J. Yewdall and P. M. Harrison, *Biochem. J.*, 1993, **296**(Pt 3), 721–728.

46 A. Treffry, Z. Zhao, M. A. Quail, J. R. Guest and P. M. Harrison, *Biochemistry*, 1995, **34**, 15204–15213.

47 L. Toussaint, M. G. Cuypers, L. Bertrand, L. Hue, C. V. Romao, L. M. Saraiva, M. Teixeira, W. Meyer-Klaucke, M. C. Feiters and R. R. Crichton, *J. Biol. Inorg. Chem.*, 2009, **14**, 35–49.

48 C. Pozzi, F. Di Pisa, C. Bernacchioni, S. Ciambellotti, P. Turano and S. Mangani, *Acta Crystallogr., Sect. D: Biol. Crystallogr.*, 2015, **71**, 1909–1920.

49 F. Bou-Abdallah, G. Biasiotto, P. Arosio and N. D. Chasteen, *Biochemistry*, 2004, **43**, 4332–4337.

50 P. Santambrogio, S. Levi, A. Cozzi, B. Corsi and P. Arosio, *Biochem. J.*, 1996, **314**, 139–144.

51 M. R. Hasan, T. Tosha and E. C. Theil, *J. Biol. Chem.*, 2008, **283**, 31394–31400.

52 S. Levi, S. J. Yewdall, P. M. Harrison, P. Santambrogio, A. Cozzi, E. Rovida, A. Albertini and P. Arosio, *Biochem. J.*, 1992, **288**, 591–596.

53 K. D. Welch, C. A. Reilly and S. D. Aust, *Free Radicals Biol. Med.*, 2002, **33**, 399–408.

54 X. Liu and E. C. Theil, *Proc. Natl. Acad. Sci. U. S. A.*, 2004, **101**, 8557–8562.

55 F. Bou-Abdallah, G. Zhao, H. R. Mayne, P. Arosio and N. D. Chasteen, *J. Am. Chem. Soc.*, 2005, **127**, 3885–3893.

56 E. C. Theil, T. Tosha and R. K. Behera, *Acc. Chem. Res.*, 2016, **49**, 784–791.

57 F. Bou-Abdallah, N. Flint, T. Wilkinson, S. Salim, A. K. Srivastava, M. Poli, P. Arosio and A. Melman, *Metallomics*, 2019, **11**, 774–783.

58 D. M. Lawson, A. Treffry, P. J. Artymiuk, P. M. Harrison, S. J. Yewdall, A. Luzzago, G. Cesareni, S. Levi and P. Arosio, *FEBS Lett.*, 1989, **254**, 207–210.

59 X. Li, L. Qiu, P. Zhu, X. Tao, T. Imanaka, J. Zhao, Y. Huang, Y. Tu and X. Cao, *Small*, 2012, **8**, 2505–2514.

60 L. Li, C. J. Fang, J. C. Ryan, E. C. Niemi, J. A. Lebron, P. J. Bjorkman, H. Arase, F. M. Torti, S. V. Torti, M. C. Nakamura and W. E. Seaman, *Proc. Natl. Acad. Sci. U. S. A.*, 2010, **107**, 3505–3510.

61 E. Ryschich, G. Huszty, H. P. Knaebel, M. Hartel, M. W. Buchler and J. Schmidt, *Eur. J. Cancer*, 2004, **40**, 1418–1422.

62 M. Liang, K. Fan, M. Zhou, D. Duan, J. Zheng, D. Yang, J. Feng and X. Yan, *Proc. Natl. Acad. Sci. U. S. A.*, 2014, **111**, 14900–14905.

63 J. C. Cutrin, S. G. Crich, D. Burghelea, W. Dastru and S. Aime, *Mol. Pharm.*, 2013, **10**, 2079–2085.

64 E. Falvo, E. Tremante, R. Fraioli, C. Leonetti, C. Zamparelli, A. Boffi, V. Morea, P. Ceci and P. Giacomini, *Nanoscale*, 2013, **5**, 12278–12285.

65 D. Belletti, F. Pederzoli, F. Forni, M. A. Vandelli, G. Tosi and B. Ruozi, *Expert Opin. Drug Delivery*, 2017, **14**, 825–840.

66 J. C. Zang, H. Chen, G. H. Zhao, F. D. Wang and F. Z. Ren, *Crit. Rev. Food Sci. Nutr.*, 2017, **57**, 3673–3683.

67 B. Chiou and J. R. Connor, *Pharmaceuticals*, 2018, **11**, 124.

68 B. Jiang, L. Yan, J. Zhang, M. Zhou, G. Shi, X. Tian, K. Fan, C. Hao and X. Yan, *ACS Appl. Mater. Interfaces*, 2019, **11**, 9747–9755.

69 B. Jiang, R. Zhang, J. Zhang, Y. Hou, X. Chen, M. Zhou, X. Tian, C. Hao, K. Fan and X. Yan, *Theranostics*, 2019, **9**, 2167–2182.

70 J. O. Jeon, S. Kim, E. Choi, K. Shin, K. Cha, I. S. So, S. J. Kim, E. Jun, D. Kim, H. J. Ahn, B. H. Lee, S. H. Lee and I. S. Kim, *ACS Nano*, 2013, **7**, 7462–7471.

71 S. Kim, J. O. Jeon, E. Jun, J. Jee, H. K. Jung, B. H. Lee, I. S. Kim and S. Kim, *Biomacromolecules*, 2016, **17**, 1150–1159.

72 S. Kim, G. S. Kim, J. Seo, G. Gowri Rangaswamy, I. S. So, R. W. Park, B. H. Lee and I. S. Kim, *Biomacromolecules*, 2016, **17**, 12–19.

73 K. Fan, B. Jiang, Z. Guan, J. He, D. Yang, N. Xie, G. Nie, C. Xie and X. Yan, *Anal. Chem.*, 2018, **90**, 5671–5677.

74 M. Kanekiyo, C. J. Wei, H. M. Yassine, P. M. McTamney, J. C. Boyington, J. R. Whittle, S. S. Rao, W. P. Kong, L. Wang and G. J. Nabel, *Nature*, 2013, **499**, 102–106.

75 R. Jurado, J. Adamcik, M. Lopez-Haro, J. A. Gonzalez-Vera, A. Ruiz-Arias, A. Sanchez-Ferrer, R. Cuesta, J. M. Dominguez-Vera, J. J. Calvino, A. Orte, R. Mezzenga and N. Galvez, *J. Am. Chem. Soc.*, 2019, **141**, 1606–1613.

76 J. Zang, H. Chen, X. Zhang, C. Zhang, J. Guo, M. Du and G. Zhao, *Nat. Commun.*, 2019, **10**, 778.

77 K. Sliepen, G. Ozorowski, J. A. Burger, T. van Montfort, M. Stunnenberg, C. LaBranche, D. C. Montefiori, J. P. Moore, A. B. Ward and R. W. Sanders, *Retrovirology*, 2015, **12**, 82.

78 L. He, N. de Val, C. D. Morris, N. Vora, T. C. Thinnes, L. Kong, P. Azadnia, D. Sok, B. Zhou, D. R. Burton, I. A. Wilson, D. Nemazee, A. B. Ward and J. Zhu, *Nat. Commun.*, 2016, **7**, 12041.

79 J. Marcandalli, B. Fiala, S. Ols, M. Perotti, W. de van der Schueren, J. Snijder, E. Hodge, M. Benhaim, R. Ravichandran, L. Carter, W. Sheffler, L. Brunner, M. Lawrenz, P. Dubois, A. Lanzavecchia, F. Sallusto, K. K. Lee, D. Veesler, C. E. Correnti, L. J. Stewart, D. Baker, K. Lore, L. Perez and N. P. King, *Cell*, 2019, **176**, 1420–1431.

80 W. Ge, Y. Li, Z. S. Li, S. H. Zhang, Y. J. Sun, P. Z. Hu, X. M. Wang, Y. Huang, S. Y. Si, X. M. Zhang and Y. F. Sui, *Cancer Immunol. Immunother.*, 2009, **58**, 201–208.

81 N. M. Molino, M. Neek, J. A. Tucker, E. L. Nelson and S. W. Wang, *ACS Biomater. Sci. Eng.*, 2017, **3**, 496–501.

82 Z. Yin, S. Chowdhury, C. McKay, C. Baniel, W. S. Wright, P. Bentley, K. Kaczanowska, J. C. Gildersleeve, M. G. Finn, L. BenMohamed and X. Huang, *ACS Chem. Biol.*, 2015, **10**, 2364–2372.